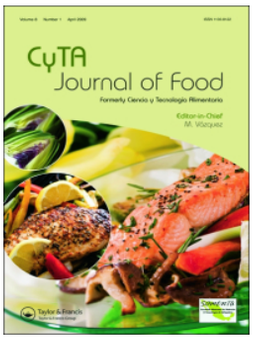

CyTA - Journal of Food

ISSN: (Print) (Online) Journal homepage: https://www.tandfonline.com/loi/tcyt20

Development of edible gelatin composite films enriched with polyphenol loaded nanoemulsions as chicken meat packaging material

Muhammad Rehan Khan, Muhammad Bilal Sadiq & Zaffar Mehmood

To cite this article: Muhammad Rehan Khan, Muhammad Bilal Sadiq & Zaffar Mehmood (2020) Development of edible gelatin composite films enriched with polyphenol loaded nanoemulsions as chicken meat packaging material, CyTA - Journal of Food, 18:1, 137-146, DOI: 10.1080/19476337.2020.1720826

To link to this article: https://doi.org/10.1080/19476337.2020.1720826

CYTA – JOURNAL OF FOOD
2020, VOL. 18, NO. 1, 137–146
https://doi.org/10.1080/19476337.2020.1720826

Development of edible gelatin composite films enriched with polyphenol loaded nanoemulsions as chicken meat packaging material

Muhammad Rehan Khan, Muhammad Bilal Sadiq and Zaffar Mehmood

School of Life Sciences, Forman Christian College (A Chartered University), Lahore, Pakistan

ABSTRACT

In this study, food grade nanoemulsions (NEs) were prepared with polyphenols (curcumin, gallic acid and quercetin); NEs were incorporated into the film forming solution at various concentrations (5%, 10% and 20% v/w of gelatin plus carrageenan). Moisture content and water solubility of film samples decreased with increasing NE concentration. Curcumin NE-loaded gelatin composite films exhibited highest antioxidant activity (27.20 ± 0.02, 45.9 ± 0 and 60.51 ± 0.36%) at 5%, 10% and 20% NE concentrations, respectively. Curcumin NE-loaded composite gelatin films also exhibited antimicrobial activity against both *Salmonella typhimurium* (6.97 ± 0.03 mm) and *Escherichia coli* (7.47 ± 0.09 mm). The chemical finger printing of films was evaluated by Fourier-transform infrared spectroscopy. Curcumin NE-loaded films showed excellent results by increasing the shelf-life of fresh broiler meat up to 17 days in comparison to control (10 days), hence can be used as alternative to conventional packaging.

ARTICLE HISTORY
Received 30 October 2019
Accepted 20 January 2020

KEYWORDS
Biodegradable; antimicrobial packaging; composite films; preservation; shelf-life

PALABRAS CLAVE
biodegradable; embalaje antimicrobiano; películas compuestas; preservación; vida útil

Desarrollo de películas compuestas de gelatina comestible enriquecidas con nanoemulsiones cargadas de polifenoles como material para el envasado de carne de pollo

RESUMEN

Para el presente estudio se prepararon nanoemulsiones (NE) de grado alimenticio con polifenoles (curcumina, ácido gálico y quercetina). Estas se incorporaron a una solución formadora de película (FFS) en varias concentraciones (5, 10 y 20% v/p de gelatina más carragenano). El contenido de humedad y la solubilidad en agua de las muestras de película disminuyeron al aumentar la concentración de NE. Las películas compuestas de gelatina cargadas con NE de curcumina exhibieron la mayor actividad antioxidante (27.20±0.02, 45.9±0 y 60.51±0.36%) a concentraciones de 5, 10 y 20% de NE, respectivamente. Asimismo, las películas de gelatina compuesta cargadas con NE de curcumina mostraron actividad antimicrobiana contra *Salmonella typhimurium* (6.97±0.03 mm) y *E. coli* (7.47±0.09 mm). La huella química de las películas fue evaluada mediante FTIR. Las películas cargadas de NE de curcumina mostraron excelentes resultados, aumentando la vida útil de la carne fresca de pollos de engorde hasta 17 días, en comparación con la del control (10 días). Por lo tanto, dichas películas pueden ser usadas como alternativa al empaque convencional.

1. Introduction

Food-borne diseases are an emerging issue for global public health and occur as a result of food-borne contaminations. Food-borne diseases can lead to hospitalization and even death can occur (Espitia, Otoni, & Soares, 2016). Annually, 600 million illnesses and 0.42 million deaths have been reported worldwide due to food-borne diseases (World Health Organization [WHO], 2015). The most common pathogens causing food-borne diseases are *Salmonella, Escherichia coli, Listeria* and *Campylobacter* spp. (Ahmed et al., 2018; Oussalah, Caillet, Saucier, & Lacroix, 2007; Trimoulinard et al., 2017). The poor handling and consumption of raw and undercooked poultry and other meats are major factors responsible for food-borne diseases (Ahmed et al., 2018). Various strategies have been opted to control the food-borne diseases; however, development of active food packaging materials not only ensures food safety but enhances the shelf-life of the perishable food products (Espitia et al., 2016). The active packaging materials, i.e., antimicrobial packaging, inhibit the growth of microbes due to controlled release of entrapped bioactive compounds (Ahmed et al., 2018). The demand for natural antimicrobials has been increased due to health hazards associated with synthetic antimicrobials (Sadiq, Hanpithakpong, Tarning, & Anal, 2015).

Due to environmental hazards, the petrochemical-based food packaging materials are being replaced by biopolymer-based biodegradable packaging (Cazón, Vázquez, & Velazquez, 2018, 2019). Gelatin is a protein-based biopolymer obtained from skin and bones of animals (i.e. bovine, porcine, poultry and fish) and widely used for the formulation of edible packaging films in food industry (Hanani, Roos, & Kerry, 2014). Lipids have been added into the protein-based film forming solutions (FFSs) to encapsulate bioactive lipophilic compounds to impart antibacterial and antioxidant activities with an aim to enhance shelf-life of food commodities (Dammak, De Carvalho, Trindade, Lourenço, & Do Amaral Sobral, 2017). Kanmani and Rhim (2014) developed gelatin-

CONTACT Zaffar Mehmood zaffarmehmood@fccollege.edu.pk; zaffar777@yahoo.com School of Life Sciences, Forman Christian College (A Chartered University), Lahore 54600, Pakistan

Supplemental data for this article can be accessed Publisher's website

based nanocomposite films with potent antimicrobial activity of silver nanoparticles (NP) against various food-borne pathogens. Nanotechnology is a rapidly growing field to produce materials at a nanoscale (20–200 nm diameter), especially for food packaging applications (Borum & Güneş, 2018). The antibacterial activity of phenolic compounds is directly related to their structure and the target microbe (Skroza et al., 2019). Phenolic compounds are capable of interacting with cellular organelles of bacteria thus altering or inhibiting their functions (Skroza et al., 2019). The phenolic compounds from edible plants have been frequently used for food preservation due to their antioxidant and antimicrobial characteristics. Curcumin is a phenolic compound derived from turmeric (*Curcuma longa*) plant that have been reported to possess strong antioxidant, anti-inflammatory and antimicrobial activities (Infante, Chowdhury, Nimmanapalli, & Reddy, 2014). It has been reported that mono-carbonyl analogues of curcumin are potent antimicrobials against food-borne pathogens (Tajbakhsh et al., 2008). Quercetin has been reported to inhibit the growth of *E. coli* by binding with GyrB subunit of *E. coli* DNA gyrase, thus inhibiting the ATPase activity of the enzyme (Cushnie & Lamb, 2005).

In this study, gelatin-based edible composite films were developed by incorporating polyphenol (curcumin and quercetin)-based nanoemulsion (NE) to enhance the shelf-life of fresh broiler meat.

2. Materials and methods

2.1. Preparation and characterization of NEs

The oil phase was prepared by homogenizing (495 g for 5 min, Ultra-Turrax IKA T25, Wasserburg, Bodensee, Germany) various concentrations (10–30 mg) of curcumin and quercetin (Sigma-Aldrich, USA), in sunflower oil (5% and 10% v/v, separately) (Sigma-Aldrich, USA) at 25°C. The aqueous phase was prepared by dissolving surfactant (Hi-cap 100, 2.5% and 5% w/v) (Ingredion, Humberg, Germany) in distilled water under stirring overnight by using magnetic stirrer (PCE-MSR 300, PCE Instruments, UK) at 25°C. In case of NEs encapsulated with gallic acid, different concentrations (10–30 mg) of gallic acid were dispersed separately in aqueous phase (Tables S1–S3, supplementary material).

Oil-in-water NEs were prepared by adding polyphenols (i.e. curcumin, quercetin and gallic acid) (Sigma-Aldrich, USA) at 10–30 mg concentration into 100 mL of emulsion along with 5–10% v/v sunflower oil (Sigma-Aldrich, USA), 2.5–5% w/v Hi-Cap 100 (Ingredion, Humberg, Germany) in distilled water by using a two-step homogenization method (Dammak & Sobral, 2019). Briefly, a coarse emulsion was prepared by homogenizing the mixture at 495 g for 5 min by using a rotor-stator homogenizer. Second, fine emulsion was obtained by passing the coarse emulsion through high pressure homogenizer (Model L-HM2, HOMMAK, Izmir, Turkey) at homogenizer pressure (60–120 MPa), for three cycles.

NE stability was measured by either heating the samples at 80°C for 30 min or by centrifuging them at 1235 × *g* for 30 min at 5°C (Sari et al., 2015). Stable NE samples were then characterized through Zetasizer Nano ZS90 (Malvern Co., UK) by using dynamic light scattering method to determine particle size distribution. Zeta-potential on the oil droplets in the emulsion was determined at 25°C and 3.9 V along with PDI (polydispersity index).

2.2. Determination of encapsulation efficiency

The encapsulation efficiency of NE was determined by method given by Sari et al. (2015) with slight modifications. NEs were passed through vivaspin concentrators of molecular weight cutoff) 100 kDa and centrifuged for 30 min at 1235 × *g* and 5° C. The encapsulation efficiency was calculated by measuring the total phenolic content (TPC) of the collected permeate. TPC of permeate and NEs was then analyzed by Folin–Ciocalteu's method (Zheng & Wang, 2001).

2.3. Preparation of gelatin composite films

Single and composite gelatin films were prepared by solution casting method. Briefly, FFS was prepared by dissolving different concentrations (6.5%, 7%, 7.5% and 8%, w/v) of bovine gelatin (Sigma-Aldrich, USA) and carrageenan (Sigma-Aldrich, USA) (0.5%, 1% and 1.5%, w/v) in distilled water (Table 2). Glycerol was used as plasticizer (Sigma-Aldrich, USA) (0.15 g of glycerol per gram of gelatin for single gelatin films and 0.15 g of glycerol per gram of combined mixture of gelatin and carrageenan for composite films). FFS was homogenized by mixing for an hour at 45°C and 150 rpm in shaking incubator (Wisecube, Korea).

NE-loaded gelatin composite films were prepared by adding NEs at various concentrations (5%, 10% and 20% by weight of gelatin plus carrageenan) into FFS and by homogenizing the FFS at 6000 rpm for 5 min. FFS was finally sonicated by high intensity ultrasonic processor (Heidolph, Germany) for 15 min to remove air bubbles and casted on polystyrene petri plates and allowed to dry in the oven (Memmert, ULM 500, Germany) for 15–18 h at 45°C (Dammak et al., 2017). Before characterization, all the films were conditioned at 25°C and relative humidity of 57% ± 1 for 3 days.

2.4. Characterization of films

2.4.1. Film thickness

The thickness of the films was measured by using a hand-held micrometer screw gauge (ID-C112PM, Mitutoyo, Japan) with an accuracy of 0.01 mm.

2.4.2. Mechanical properties of films

Tensile strength (TS), elastic modulus (EM) and elongation at break (EAB) of the film samples were determined according to the standard ASTM D822-09 method by using a universal testing machine (Model 5565, Instron Engineering Corporation, USA) in tensile mode. Mechanical cross-head speed and initial grip separation were set at 5 mm min^{-1} and 40 mm, respectively, with a load cell of 500 N.

2.4.3. Moisture content and water solubility

The moisture content (MC) was measured by cutting the film samples into strips and dried in an oven (Memmert ULM 500, Germany) for 24 h at 100°C. The weight of the film samples was measured before and after drying. The weight loss was expressed as MC in terms of percentage.

The water solubility (WS) of film samples was measured by method given by Gontard and Guilbert (1994) and Wang, Liu, Holmes, Kerry and Kerry (2007) with slight modifications. Briefly, the film was cut into small strips and dried in an oven at 100°C for 24 h to constant weight. After drying, each sample was immersed in distilled water (100 mL) for 24 h followed by the removal from solution and dried again for

24 h at 100°C. Final weights were used to calculate the WS of film by using the following equation:

$$\text{Water solubility(WS)\%} = \frac{(\textit{initial weight} - \textit{final weight})}{\text{intial weight}} \times 100 \quad (1)$$

2.4.4. Water vapor permeability

The water vapor permeability (WVP) of gelatin films was determined according to standard ASTM E96 gravimetrically. Film samples (5.3 cm in diameter) were placed inside silica gel containing aluminum cells (0% relative humidity) in a desiccator containing distilled water (100% relative humidity) at 30°C. Finally, to ensure steady-state permeation, aluminum cells were weighed (±0.01 g) for 10 days daily. WVP was calculated by using following equation:

$$WVP = \frac{\Delta g}{\Delta t}\left(\frac{x}{A.\Delta P}\right) \quad (2)$$

where $\Delta g/\Delta t$ is the rate of change of weight (g h^{-1}), x represents sample thickness (mm), A is the area of permeation, and ΔP (4245 Pa) is the difference of partial pressure across the film samples.

2.4.5. Total color difference and transparency of film samples

Total color difference of the films was measured as compared to standard white plate with hunter color values (L^* = 97.75, a^* = −0.49 and b^* = 1.96) with chroma meter (Minolta, CR200b, Japan). The average value was taken from nine replicates of each sample for hunter color coordinates (CIE L^*, a^* and b^*). The difference in color (ΔE) was calculated by using the following equation:

$$\Delta E^* = \left[(\Delta L^*)^2 + (\Delta a^*)^2 + (\Delta b^*)^2\right]^{0.5} \quad (3)$$

where ΔL^*, Δa^* and Δb^* are the differences of color parameter between white standard and film samples.

Transparency was expressed as percent transmittance for each film sample measured at 280 and 660 nm, respectively, by UV–vis spectrophotometer (Model 8451A, Hewlett-Packard Co., CA, USA). The film samples were cut into rectangular pieces and were clamped between magnetic cell holders of spectrophotometer and readings were read (Kanmani & Rhim, 2014). The measurements were taken in triplicates and average values were presented.

2.5. Antioxidant activity

Antioxidant activity of the composite films was measured in terms of DPPH% (2,2-diphenyl-1-picrylhydrazyl) (Sigma-Aldrich, USA) inhibition by a method given by Sadiq et al. (2015) with slight modifications. Film samples were cut into 4 × 4 cm size strips and were added into freshly prepared 5 mL of methanol solution of DPPH (40 mg L^{-1}); the mixture was kept in dark place for 30 min at 25°C. After 30 min of incubation, the absorbance was read at 517 nm against blank for each mixture. Ascorbic acid (Sigma-Aldrich, USA) was taken as positive control. Percentage inhibition was calculated by using the following equation:

$$DPPH\%\ inhibition = \frac{(AC - AS)}{AC} \times 100 \quad (4)$$

AC is the absorbance of control and AS is absorbance of sample.

2.6. Antibacterial activity of film samples

Antibacterial activity of films was determined by agar diffusion assay as described by Iamareerat, Singh, Sadiq and Anal (2018). The composite films were cut into 4 mm disks and placed on the surface of Mueller–Hinton agar plates inoculated with *Salmonella typhimurium* ATCC 14028 and *E. coli* ATCC 8739. The agar plates were than incubated at 37°C for 24 h and antibacterial activity was evaluated by measuring zone of inhibition (ZI).

2.7. Fourier-transform infrared spectroscopy

Fourier-transform infrared spectra of gelatin films were analyzed by using Fourier-transform infrared spectroscopy (FT-IR) spectroscopy instrument (Model: Cary 630, Agilent technologies, Santa Clara, CA, USA) equipped with a universal attenuator total reflectance accessory. The spectra were recorded in the range of 4000–650 cm^{-1} with a resolution of 4 cm^{-1}, using absorbance mode. Film samples (1 cm^2) were placed horizontally on the spectrometer, and for each spectrum, 100 scans were co-added.

2.8. Influence of NE-loaded gelatin composite films on shelf-life of raw broiler meat

Film samples with best antioxidant and antibacterial properties were selected for packaging of broiler meat. Film samples were cut into 6 × 6 cm squares. Three sides of two sheets of the film were sealed to pack fresh meat (8 g). The last side was also sealed to completely close the packaging. The fresh broiler meat was stored at refrigeration temperature (4°C), and the quality of the meat was evaluated every day.

2.8.1. Microbiological analysis

Meat samples at each interval of time were mixed with 0.1% of peptone water and shredded in a stomacher (Stomacher 400, Lab. Blender, UK). After the preparation of series of dilutions, 0.1 mL of each dilution was spread on plate count agar containing plate and incubated for 24 h at 37°C. Total colonies were counted and represented as CFU g^{-1} broiler meat (Iamareerat et al., 2018).

2.8.2. Determination of pH

pH of the meat samples was measured by homogenizing meat sample (10 g) with 100 mL distilled water for 1 min by using a pH meter (Inolab, Mexico) (Takma & Korel, 2019).

2.9. Statistical analysis

All experiments were performed in triplicates; however, the color attributes were estimated in nine replicates. One-way analysis of variance was performed to estimate the significant differences ($p < 0.05$) between means observations by using SPSS statistical software package (SPSS, version 23.0, Inc., Chicago, IL, USA).

3. Results and discussion

3.1. Preparation and characterization of NEs

Different concentrations of both core (oil and polyphenols) materials and Hi-Cap 100 were used to optimize stable formulations. Stable formulations were obtained at 10% v/v sunflower oil, 5% w/v of Hi-Cap 100 and with 10 mg of polyphenolic compounds, i.e. curcumin, quercetin and gallic acid as shown in Table 1.

The most stable formulation was obtained with 10% v/v sunflower oil and 5% w/v of Hi-Cap 100 with a storage stability of 135 ± 0 days at 25°C having a particle size of 98.21 ± 0.36 nm, zeta-potential of −28.1 ± 0.05 mV and PDI of 0.328 ± 0.0006. PDI can be used as a measure of size distribution. When PDI value is less than 0.1, it is an indication of monodisperse size distribution while higher PDI (>0.2) value indicates heterogeneity. The lower value of PDI can be correlated with more stability on storage. The surface charge of the emulsion particles is roughly characterized by the zeta-potential of emulsions.

Low storage stability of polyphenol encapsulated NE can be attributed to their lower zeta-potential values as compared to NE without polyphenols (NEWP). The lower zeta-potential and smaller particle size can be attributed to the higher quantity of (i.e. 5% w/v Hi-Cap) used in the formulations. NEs have been prepared with high surfactant quantities, i.e. tween and span (Sari et al., 2015). In this present study, NE samples prepared with sunflower oil showed a mean particle size range below 100 nm due to higher amount of surfactant which can cover oil droplets in oil phase and thus lowers the interfacial surface tension as a result of high pressure homogenization through the breakdown of droplets (Jafari, Assadpoor, He, & Bhandari, 2008).

An improvement in physical stability can be observed with higher zeta-potential values which lead to repulsive forces among particles in a multiphase system. Since fatty acids are the building blocks for fats, the carboxylic acid groups of fatty acids are responsible for negative charge on particles (Sood, Jain, & Gowthamarajan, 2014). Bhargava, Conti, Da Rocha and Zhang (2015) reported negatively charged oregano oil NEs with average zeta-potential of −18 mV. Sari et al. (2015) reported curcumin NEs with an average droplet size of 141.6 nm, zeta-potential of −6.9 mV and a PDI value of 0.273.

3.2. Encapsulation efficiency

Folin–Ciocalteu assay based on oxidation-reduction was used to measure the TPC of the NE. The encapsulation efficiency was calculated by taking the total polyphenolic content in NE as marker. The encapsulation efficiency was found maximum for quercetin being a lipophilic compound at 92.58 ± 0.001% as shown in Table 1.

Encapsulation efficiency of curcumin in NE found in this study (90.36 ± 0.002%) was in accordance with the results of Mohanty and Sahoo (2010) with entrapment efficiency of (90 ± 2.55%), and 90.56 ± 0.47% reported by Sari et al. (2015). The encapsulation efficiency for quercetin was reported to vary from 56% to 92% with the increase in pH from 4 to 9 (Son et al., 2019). In this study, encapsulation efficiency for quercetin was found to be 92.58 ± 0.001%, while due to hydrophilic nature of gallic acid, low encapsulation efficiency 86.85 ± 0.3 was found in this study.

3.3. Characterization of gelatin films

The results for characterization of film samples are shown in Table 2. After the preparation of composite film samples of gelatin and carrageenan at various concentrations, FFS containing 7.5 g gelatin and 0.5 g carrageenan were selected for incorporation of NE into the FFS at various concentrations (5%, 10% and 20%) based on results of physicochemical properties of gelatin films.

3.3.1. Thickness of film samples

Thickness of the film samples remained relatively constant even with different concentrations of NEs showed in Table 2. This might be due to the fact that film thickness is only influenced by solid content of solution used for film development along with low volume of oil (dispersed phase) incorporated into NE, which represents 10% v/v of NE. Thus, the film thickness ranged from 0.49 to 0.527 mm. Dammak et al. (2017) reported the similar trends for film thickness of rutin NE-loaded gelatin films ranged between 0.082 and 0.086 mm. It has been reported that only solid content in the FFS influences the thickness of the film samples (Dammak et al., 2017). Film thickness in this experiment was found relatively constant after the incorporation of NE into the FFS. Similar results were observed upon incorporation of thyme oil in chitosan films (Altiok, Altiok, & Tihminlioglu, 2010).

3.3.2. Mechanical properties of film

For gelatin composite films loaded with NEs, TS, EAB and EM were increased linearly with increasing content of NEs (5–-20%) in FFS (Table 2). Thus, contrarily to the behavior regarding plasticizer effect, TS can be represented as a linear function of EAB (Dammak et al., 2017). These results

Table 1. Formulation of food grade NEs, their characterization and encapsulation efficiency.

Tabla 1. Formulación de NE de grado alimenticio, caracterización y eficiencia de encapsulación del mismo.

Composition of nanoemulsions	Storage stability (days)	Particle size (nm)	Zeta-potential (mV)	Polydispersity index	Encapsulation efficiency (%)
Sunflower oil 10% + Hi-cap 5%	135 ± 0^{a}	98.21 ± 0.36^{a}	−28.1 ± 0.05^{a}	0.328 ± 0.0^{a}	–
Sunflower oil 10% + Hi-cap 5% + curcumin 10 mg	96 ± 2^{b}	88.45 ± 4.38^{b}	−26.34 ± 0.12^{c}	0.19 ± 0.0^{c}	90.36 ± 0.0
Sunflower oil 10% + Hi-cap 5% + gallic acid 10 mg	61 ± 1^{d}	97.64 ± 1.82^{a}	−21.33 ± 0.20^{d}	0.2 ± 0.0^{b}	86.85 ± 0.3
Sunflower oil 10% + Hi-cap 5% + quercetin 10 mg	73 ± 0^{c}	94.25 ± 0.94^{ab}	−27.1 ± 0.1^{b}	0.20 ± 0.0^{b}	92.58 ± 0.0

Different superscript letters (a–d) within a column indicate significant ($p < 0.05$) differences among mean observations.

Las distintas letras de superíndice (a-d) dentro de una columna indican la presencia de diferencias significativas ($p < 0.05$) entre las observaciones medias.

Table 2. Characterization of edible gelatin composite film samples.

Tabla 2. Caracterización de muestras de película compuesta de gelatina comestible.

Film composition	TS (MPa)	EAB (%)	EM (MPa)	Thickness (mm)	Moisture content (MC%)	Water solubility (WS %)	WVP ($\times 10^{-10}$ g s^{-1} m^{-1} Pa^{-1})	Total color difference (ΔE)	$T_{280\ nm}$ (%)	$T_{660\ nm}$ (%)
G 8 g	9.81 ± 0.20^{d}	41.02 ± 1.40^{d}	103.02 ± 1.90^{a}	0.426 ± 0.005^{g}	13.10 ± 0.01^{a}	61.09 ± 0.02^{a}	12.37 ± 0.05^{j}	2.07 ± 0.01^{l}	68.31 ± 0^{a}	86.41 ± 0.42^{a}
G 7.5 g + C 0.5 g	11.09 ± 0.57^{d}	44.32 ± 1.27^{d}	106.49 ± 1.01^{a}	0.433 ± 0.005^{g}	12.81 ± 0.02^{b}	61.01 ± 0.005^{b}	12.63 ± 0.02^{j}	6.28 ± 0.05^{k}	67.39 ± 0.005^{b}	85.22 ± 0.01^{bcd}
G 7 g + C 1 g	10.96 ± 0.12^{d}	44.16 ± 0.87^{d}	105.23 ± 0.75^{a}	0.433 ± 0.002^{g}	12.76 ± 0.015^{c}	60.98 ± 0.011^{b}	12.69 ± 0.005^{j}	6.46 ± 0.02^{k}	67.16 ± 0.04^{c}	85.86 ± 0.05^{ab}
G 6.5 g + C 1.5 g	10.78 ± 0.11^{d}	44.16 ± 1.06^{d}	105.06 ± 0.15^{a}	0.463 ± 0.005^{f}	12.77 ± 0.02^{bc}	60.99 ± 0.015^{b}	12.68 ± 0.02^{j}	6.93 ± 0.015^{j}	66.98 ± 0.01^{d}	85.79 ± 0.01^{abc}
G 7.5 g + C 0.5 g + NEWP 20%	33.96 ± 1.39^{a}	70.65 ± 0.55^{a}	142.17 ± 2.58^{a}	0.501 ± 0^{bcd}	5.73 ± 0.01^{kl}	47.12 ± 0.01^{j}	20.77 ± 0.18^{b}	15.21 ± 0.005^{d}	52.33 ± 0.017^{k}	74.88 ± 0.19^{f}
G 7.5 g + C 0.5 g + NEWP 10%	25.7 ± 1.41^{b}	59.34 ± 2.40^{b}	123.59 ± 3.15^{b}	0.501 ± 0.001^{bcd}	8.12 ± 0.015^{g}	54.66 ± 0.02^{h}	16.44 ± 0.15^{f}	11.68 ± 0.25^{f}	59.53 ± 0.02^{h}	79.33 ± 0.56^{e}
G 7.5 g + C 0.5 g + NEWP 5%	20 ± 1.31^{c}	49.22 ± 2.96^{c}	114.51 ± 3.38^{c}	0.500 ± 0.0005^{bcd}	10.05 ± 0.02^{f}	57.09 ± 0.015^{f}	14.17 ± 0.06^{i}	9.91 ± 0.01^{h}	62.65 ± 0.015^{e}	85.08 ± 0.09^{cd}
G 7.5 g + C 0.5 g + C″ 20%	34.82 ± 0.39^{a}	73.01 ± 0.93^{a}	146.76 ± 0.96^{a}	0.507 ± 0.002^{b}	5.69 ± 0.01^{l}	46.84 ± 0.02^{k}	21.58 ± 0.41^{a}	18.12 ± 0.015^{a}	49.21 ± 0.02^{m}	72.44 ± 0.18^{h}
C 7.5 g + C 0.5 g + C″ 10%	26.27 ± 1.24^{b}	61.51 ± 2.61^{b}	124.9 ± 1.6^{b}	0.500 ± 0.001^{bcd}	8 ± 0.01^{i}	54.88 ± 0.01^{g}	17.41 ± 0.25^{e}	12.09 ± 0.005^{e}	58.63 ± 0.03^{j}	79.32 ± 0.16^{e}
G 7.5 g + C 0.5 g + C″ 5%	19.65 ± 0.76^{c}	51.11 ± 2.61^{c}	116.52 ± 1.13^{c}	0.502 ± 0.002^{bc}	10.02 ± 0.005^{f}	57.33 ± 0.03^{d}	14.48 ± 0.005^{hi}	10.27 ± 0.005^{g}	61.36 ± 0.017^{g}	84.89 ± 0.02^{d}
G 7.5 g + C 0.5 g + Q 20%	34.05 ± 1.14^{a}	72.94 ± 0.85^{a}	143.82 ± 1.27^{a}	0.496 ± 0.003^{cde}	5.74 ± 0.01^{jk}	46.76 ± 0.005^{l}	21.26 ± 0.08^{a}	15.79 ± 0.02^{b}	52.08 ± 0.02^{l}	73.91 ± 0.6^{g}
G 7.5 g + C 0.5 g + Q 10%	25.95 ± 1.16^{b}	60.61 ± 0.33^{b}	123.82 ± 0.56^{b}	0.49 ± 0.001^{e}	8.06 ± 0.005^{h}	54.37 ± 0.005^{i}	17.38 ± 0.03^{e}	11.78 ± 0.07^{f}	59.34 ± 0.015^{i}	79.96 ± 0.01^{e}
G 7.5 g + C 0.5 g + Q 5%	19.28 ± 1.12^{c}	50.8 ± 0.51^{c}	115 ± 2.64^{c}	0.492 ± 0.001d^{e}	10.11 ± 0.01^{e}	57.25 ± 0.01^{e}	14.69 ± 0.07^{gh}	9.21 ± 0.03^{i}	62.10 ± 0.005^{f}	85.08 ± 0.03^{cd}
G 7.5 g + C 0.5 g + GA 20%	34.02 ± 1.22^{a}	72.14 ± 0.85	142.78 ± 2.41^{a}	0.527 ± 0.002^{a}	5.78 ± 0.005^{j}	46.72 ± 0.005^{l}	20.33 ± 0.02^{c}	15.49 ± 0.01^{c}	52.25 ± 0.06^{k}	74.10 ± 0.03^{g}
G 7.5 g + C 0.5 g + GA 10%	25.6 ± 1.67^{b}	60.17 ± 0.16	123.73 ± 2.7^{b}	0.523 ± 0.004^{a}	8.15 ± 0.02^{g}	54.65 ± 0.015^{h}	18.01 ± 0.07^{d}	12.15 ± 0.06^{e}	59.39 ± 0.005^{i}	79.84 ± 0.07^{e}
G 7.5 g +C 0.5 g + GA 5%	19.20 ± 0.8^{c}	50.3 ± 0.4	114.63 ± 0.23^{c}	0.527 ± 0.001^{a}	10.2 ± 0.01^{d}	57.41 ± 0.02^{c}	15.07 ± 0.01^{g}	10.03 ± 0.02^{h}	62.15 ± 0.06^{f}	85.08 ± 0.037^{cd}

Different superscript letters (a–m) within a column show significant ($p < 0.05$) differences among mean observation. G defines gelatin, C defines carrageenan, NEWP defines nanoemulsions without polyphenols, C″ defines curcumin, Q defines quercetin and GA defines gallic acid. TS: Tensile strength; EAB: elongation at break; EM: elastic modulus.

Las distintas letras de superíndice (a-m) dentro de una columna indican la presencia de diferencias significativas ($p < 0.05$) entre observaciones medias. G significa gelatina; C, carragenano; NEWP, nanoemulsiones sin polifenoles; C″, curcumina; Q, quercetina; y GA, ácido gálico. TS = resistencia a la tracción, EAB = alargamiento a la rotura, EM = módulo elástico.

suggested that phenolic compounds loaded in NEs provoked a type of cross-linking among subjacent peptide molecules resulting in the development of an elastic and resistant film matrix structure; the hydroxy groups of the phenolic compounds might form a bond with hydrophobic functional groups of amino acids in gelatin structure and the binding of glycoside ring of polyphenols (curcumin, quercetin and gallic acid) with hydrophilic entities of gelatin molecule. Another possible effect of NEs might be that the oil droplets loaded with phenolics were liquid at 25°C and can enhance film flexibility due to the fact that nanoscale size can easily be deformed in the film structure (Fabra, Talens, & Chiralt, 2008). Rutin was reported to provoke a type of cross-linking among peptide molecules of gelatin, thus improving mechanical properties of gelatin films (Dammak et al., 2017). The hydroxyl groups of catechin have been reported to form multiple hydrogen bonds with the functional groups of gelatin and the interactions of hydrophobic residues of gelatin with benzopyran rings of catechin have been reported to be the major factor responsible for stabilizing the gelatin molecule (Haroun & El Toumy, 2010).

3.3.3. MC and WS

MC and WS of film samples decreased with increasing content of NE from 5% to 20% as compared to control gelatin and gelatin composite films without NE. This is due to the fact that NE inclusion in FFS enhances the hydrophobic character of the film samples. MC of the gelatin films ranged between 13% and 5% as shown in Table 2. Lowest readings for MC (5.69%) were observed for gelatin composite films loaded with 20% curcumin. The WS of film samples ranged between 46% and 61% with highest (61.09 ± 0.02%) observed for single gelatin films due to their hydrophilic nature and addition of hydrophilic plasticizer glycerol.

MC is one of the most important film characteristics which represents total molecules of water immersed in the microstructural network of composite films. Kanmani and Rhim (2014) reported increase in MC (i.e. 12.4–13.1%) of gelatin/silver nanocomposite films with increasing concentration of silver NP due to reduction of polymer chain interactions, thus increasing the availability of free hydroxyl groups by addition of silver NP to absorb water. Ma et al. (2012) reported decreased MC for gelatin/olive oil composite films with increasing concentration of olive oil, thus increasing hydrophobic character of film samples consequently lowering the protein–water interaction. Dammak et al. (2017) reported the similar trends for WS values ranged from 51% to 58%. The WS decreased with increasing content of rutin-loaded NE in the FFS due to increased hydrophobic character.

3.3.4. Water vapor permeability

WVP varied from 12 to 21 × 10^{-10} g s^{-1} m^{-1} Pa^{-1} for gelatin film samples (Table 2); an increase in WVP was observed with increasing concentration of NE shown in table. However, film samples will always be very permeable to water vapor, as these differences do not constitute key loose in the barrier properties of water vapor. Generally, a plasticizer, i.e. glycerol, reduced the intermolecular forces, as it is located between the adjacent chains of gelatin molecules, consequently favored the mobility of the polypeptide chains in the film matrix, due to increase in the free volume of the system. A substantial increase in segmental motions and free

volume might be due to increased mobility, which favors the transport of water vapor molecules through the film.

Dammak et al. (2017) observed similar trends for WVP of activated gelatin films loaded with rutin NEs ranged 12–18 × 10^{-10} g s^{-1} m^{-1} Pa^{-1}. The WVP of the gelatin films increased with increasing concentration of rutin-loaded NE in the film FFS (Dammak et al., 2017). Pranoto, Rakshit and Salokhe (2005) reported elevated values of WVP for alginate-based films due to incorporation of higher concentrations of garlic oil (0.3–0.4%) into the films. A decrease in the hydrophobic character of film matrix might be due to interaction of oil components with hydrophilic protein domains (Rodríguez, Oses, Ziani, & Mate, 2006). The WVP decreased with increasing concentration of silver NP in the gelatin films from 3.02 to 2.97 × 10^{-9} gm m^{-2} Pa^{-1} s^{-1}. The silver NP might act as discontinuous barrier for the diffusion of water vapor in the film samples (Kanmani & Rhim, 2014).

3.3.5. Total color difference and transparency

Total color difference for single gelatin film was found to be lowest (2.07 ± 0.01) amongst all film samples and it was almost transparent (a characteristic of gelatin-based films). Maximum value for total color difference (18.12 ± 0.015) was observed for gelatin composite films containing 20% curcumin NE as shown in Table 2. Hosseini, Razavi and Mousavi (2009) reported significant increase in total color difference (15–28) with incorporation of cinnamon oil in chitosan films; however, such pronounced effect was not observed with the incorporation of clove or thyme oil. Δ*E* ranged from 2.1 to 61.4 and increased linearly with increasing concentration of silver NP (i.e. from 10 to 40 mg) into gelatin films (Kanmani & Rhim, 2014). A slight increase in the Δ*E* values with gelatin films incorporated with rutin-loaded NE was reported. It has been reported that lipids influence color of gelatin films, depending upon the type and concentration of oil used (Dammak et al., 2017).

Transparency of the packaging films is one of the most important physical parameters which provides the ability to see though the packaging films or prevents light transmission through it. Table 2 is showing the values for percentage transmittance measured at 280 and 660 nm for UV and visible region, respectively. The transmittance for single gelatin film was 68.31% and 86.41% for UV and visible regions, respectively. The inclusion of polyphenol-loaded NE reduced the transmittance of composite gelatin films for UV and visible regions. This could be due to the dispersion of NE into the polymeric matrix of the film samples. Percentage transmittance decreased significantly with the increase in concentration of NE from 5% to 20%. The percentage transmittance ranged between 72% and 86%. However, Dammak et al. (2017) reported that the transparency values for all film samples stayed around 3% for all the film samples due to the use of type and concentration of oil used for NE. It has been reported that with increase in the concentration of NP, the percentage transmittance (T_{660}%) of gelatin films decreased and it varied from 49.6% to 89.1% (Kanmani & Rhim, 2014).

3.4. Antioxidant activity

A considerable variation in antioxidant potential was found for film samples at various concentrations of NE incorporated into composite films as shown in Figure 1. The highest DPPH inhibition (60.51 ± 0.36%) was found for curcumin enriched NE-loaded films at 20% NE concentration, whereas it was 58.47 ± 0.02% and 29.12 ± 0.03%, respectively, for quercetin and gallic acid. There was increase in DPPH% inhibition with increase in concentration of NEs (5–20%). The positive control ascorbic acid showed DPPH inhibition of 96.15 ± 0.25% at 1000 µg mL^{-1}. Furthermore, single gelatin (1.07 ± 0.01%), composite gelatin films without NE (1.03 ± 0%) and film samples incorporated with NEWP at 5%, 10% and 20% (1.13 ± 0.02,

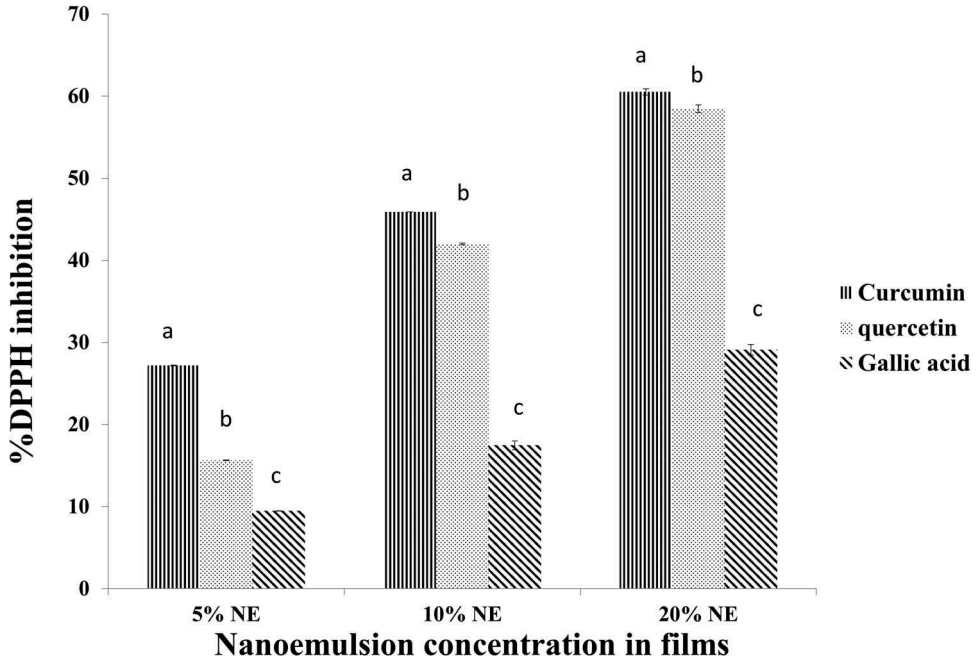

Figure 1. DPPH% inhibition for composite gelatin films containing 5%, 10% and 20% NEs. Different superscript letters (a–c) above the bars indicate significant ($p < 0.05$) differences among mean observations.

Figura 1. Porcentaje de inhibición de DPPH de películas de gelatina compuestas que contienen 5, 10 y 20% de NE. Las distintas letras de superíndice (a-c) sobre las barras indican la presencia de diferencias significativas ($p < 0.05$) entre las observaciones medias.

1.14 ± 0.03 and 1.16 ± 0%) exhibited significantly lower antioxidant activity.

Sadiq et al. (2015) reported the antioxidant potential of different parts of *Acacia nilotica* via DPPH radical scavenging activity. The lowest (33.37 ± 1.53%) and highest (91.98 ± 0.73%) DPPH inhibitions were found for bark and leaves, respectively. Dammak et al. (2017) reported DPPH radical scavenging activity of single gelatin and gelatin films loaded with rutin NEs (ranged 0.07–1.97 μg mL^{-1}). Antioxidant activity of the film samples increased with the increasing concentration of NE in FFS from 5% to 20%.

3.5. Antibacterial activity

Single gelatin, composite gelatin and composite gelatin films with NEWP were taken as control and did not present any antibacterial activity against *S. typhimurium* and *E. coli*. Composite gelatin films containing 20% curcumin NE showed maximum ZI (7.47 ± 0.09 mm) against *E. coli* and (6.97 ± 0.03 mm) against *S. typhimurium*. Composite films containing 5% gallic acid NEs did not show any zones of inhibition against both of the food-borne pathogens. Table 3 is showing the results of antimicrobial activity of composite film samples loaded with NE against *S. typhimurium* and *E. coli*.

Kanmani and Rhim (2014) reported antibacterial activity of gelatin/silver nanocomposite films against several food-borne pathogenic microbes, i.e. *Staphylococcus aureus, Bacillus cereus, E. coli* etc. Film samples having 40 mg of silver NP exhibited maximum zones of inhibition. Increase in the concentration of silver NP in the gelatin composite films resulted in higher zones of inhibition against pathogenic bacteria. *S. typhimurium* was found to be most susceptible against silver NP. Overall, gram-negative bacteria were found more susceptible to silver NP which might be due to bacterial membrane charge or thin cell wall of bacterial strains (Kanmani & Rhim, 2014). Gram-negative bacteria are coated with negatively charged outer membrane and thin peptidoglycan layer which facilities NP penetration (Kanmani & Rhim, 2014).

It has been reported that the addition of 0.3% (w/v) of aqueous curcumin extract to the cheese can cause reduction in the microbial count of *S. typhimurium* and *E. coli 0157:H7* (Zorofchian Moghadamtousi et al., 2014). Quercetin is one of the flavonoids compounds that were studied for antibacterial activity against food-borne pathogens. Quercetin actively inhibited the activity of DNA gyrase in *E. coli* (Cushnie & Lamb, 2005). There is some evidence of antibacterial influence of gallic acid on *S. aureus* strains when it prevented the coagulation of rabbit plasma by *S. aureus* strains (Akiyama, Fujii, Yamasaki, Oono, & Iwatsuki, 2001). Iamareerat et al. (2018) similarly reported highest antimicrobial activity of cassava starch films containing sodium bentonite (0.75%) and cinnamon essential oil (2.5%) against *E. coli* (15.25 ± 1.85 mm).

3.6. Fourier-transform infrared spectroscopy

FT-IR chemical finger printing was carried out to monitor the functional groups and changes in composition of film samples. All gelatin-based film samples presented major peaks in the amide region. Film samples loaded with different NE showed variations in the spectra as shown in Figure 2. Control film and film samples loaded with 20% curcumin, quercetin and gallic acid NE displayed the amide-I bands at 1632.6, 1632.6, 1630.7 and 1630.7 cm^{-1}, respectively (Muyonga, Cole, & Duodu, 2004). This amide-I vibration mode is mainly due to carbonyl (C=O) stretching vibration linked with the C–N stretch, in plane N–H bending mode and CCN deformation (Dammak et al., 2017). Shrestha, Sadiq and Anal (2018) reported amide-I region for culled banana-resistant starch and soy protein isolate in the range of 1627–1650 cm^{-1}. The characteristic bands for control film and film samples incorporated with 20% curcumin, quercetin and gallic acid NEs in amide-II bands were visible at 1546.8, 1546.8, 1543.1 and 1546.8 cm^{-1}, respectively. The spectrum of gelatin film samples (i.e. control and NE-loaded) displayed peaks arising for N–H stretching from 1543 to 1547 cm^{-1}. The characteristic bands for amide-III region were observed for gelatin/carrageenan (control), curcumin, quercetin and gallic acid 20% NE-loaded films at 1241.2, 1239.3, 1239.3 and 1241.2 cm^{-1}, respectively, representing C–N and N–H stretching. Lower amplitude at bands 1032.5, 1034.3 and 1036.2 cm^{-1} was observed due to replacement of glycerol with NE components (Karbowiak, Debeaufort, Champion, & Voilley, 2006). Broad and strong absorption peaks were observed for control and NE-loaded films in the range of 3278–3297 cm^{-1}, which indicates stretching vibration of O–H groups. Kanmani and Rhim (2014) similarly reported stretching vibration of O–H groups at 3288 cm^{-1} for gelatin/silver nanocomposite film samples.

The peaks of methylene (C–H) bend at 1451.8, 1451.8 and 1453.7 cm^{-1} for curcumin, quercetin and gallic acid, respectively, can be correlated with their antibacterial activity. The prominent peaks of methylene bend in curcumin and quercetin NE-loaded films were an evidence of their better

Table 3. Antibacterial activity of composite films loaded with NEs.

Tabla 3. Actividad antibacteriana de películas compuestas cargadas con NE.

Composition of films	Concentration of NEs	Zone of inhibition (mm)	
		Escherichia coli	*Salmonella typhimurium*
Gelatin (7.5 g) + carrageenan (0.5 g)	Curcumin NE 20%	7.47 ± 0.09^{a}	6.97 ± 0.03^{a}
	Curcumin NE 10%	5.63 ± 0.03^{d}	5.01 ± 0.01^{d}
	Curcumin NE 5%	4.18 ± 0.09^{f}	4.26 ± 0.01^{f}
	Quercetin NE 20%	7.05 ± 0.05^{b}	6.87 ± 0.005^{b}
	Quercetin NE 10%	5.96 ± 0.02^{c}	4.94 ± 0.02^{e}
	Quercetin NE 5%	5.64 ± 0.03^{d}	4.04 ± 0.01^{g}
	Gallic acid NE 20%	5.16 ± 0.028^{e}	5.15 ± 0.025^{c}
	Gallic acid NE 10%	4.29 ± 0.08^{f}	4.02 ± 0.025^{g}
	Gallic acid NE 5%	0	0

Different superscript letters (a–g) within each column indicate significant ($p < 0.05$) differences among mean observations.

Las distintas letras en superíndice (a-g) dentro de cada columna indican la presencia de diferencias significativas ($p < 0.05$) entre las observaciones medias.

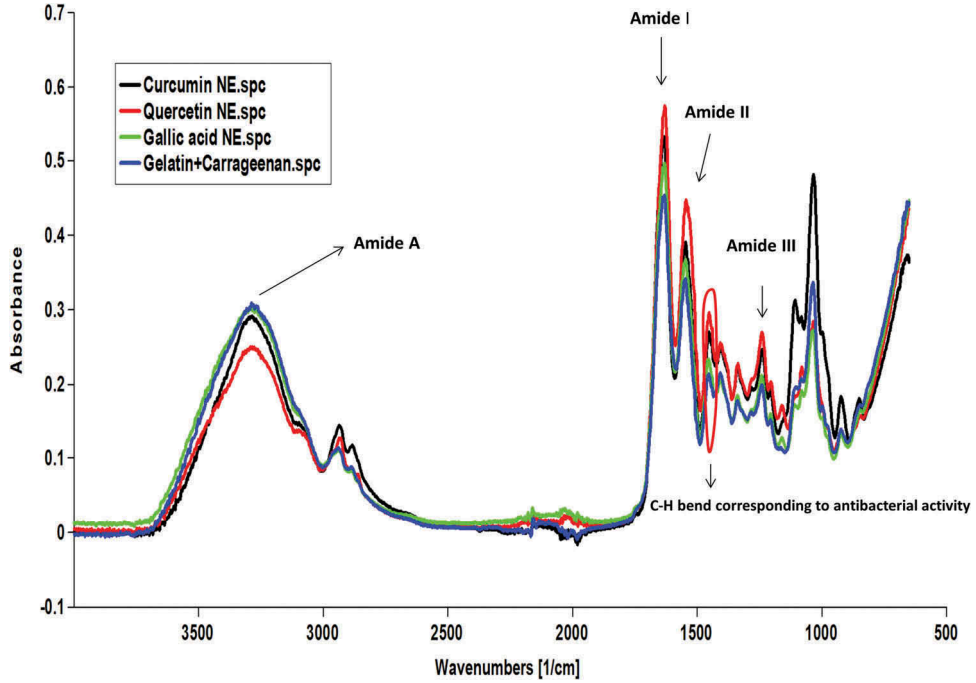

Figure 2. Fourier-transform infrared spectra of gelatin composite films incorporated with 20% NE-loaded with polyphenols.

Figura 2. Espectros infrarrojos de transformada de Fourier de películas compuestas de gelatina que incorporan 20% de NE cargado con polifenoles.

preservative potential than other films. The central methylene functional groups of curcumin might be responsible for the antibacterial activity, although less pronounced than its mono-carbonyl analogues (Liang et al., 2008).

3.7. Influence of NE-loaded gelatin composite films on shelf-life of raw broiler meat

The composite gelatin films containing 20% NE were selected for packaging of raw broiler meat at refrigeration temperature (4°C) based on their antioxidant and antibacterial activities. The selected composite films were applied as packaging to evaluate the shelf-life of meat. The influence of different types of packaging materials on the bacterial growth in broiler meat samples is shown in Figure 3. Food and Drug Administration (FDA) has set a maximum limit of 10^6 CFU g^{-1} for total plate count in meat beyond which meat should not be consumed. The broiler meat samples contained in plastic bag (control) exceed the maximum allowable level within 11 days, whereas meat packed in composite gelatin films loaded with curcumin NE remained below the maximum allowable level until 18 days. On the other hand, gallic acid NE-loaded films kept the microbial count lower than maximum allowable limit until 14 days. Therefore, NE-loaded gelatin composite films showed antimicrobial efficacy by lowering the growth of microbes. Iamareerat et al. (2018) similarly used this method to extend the shelf-life of pork meat balls by

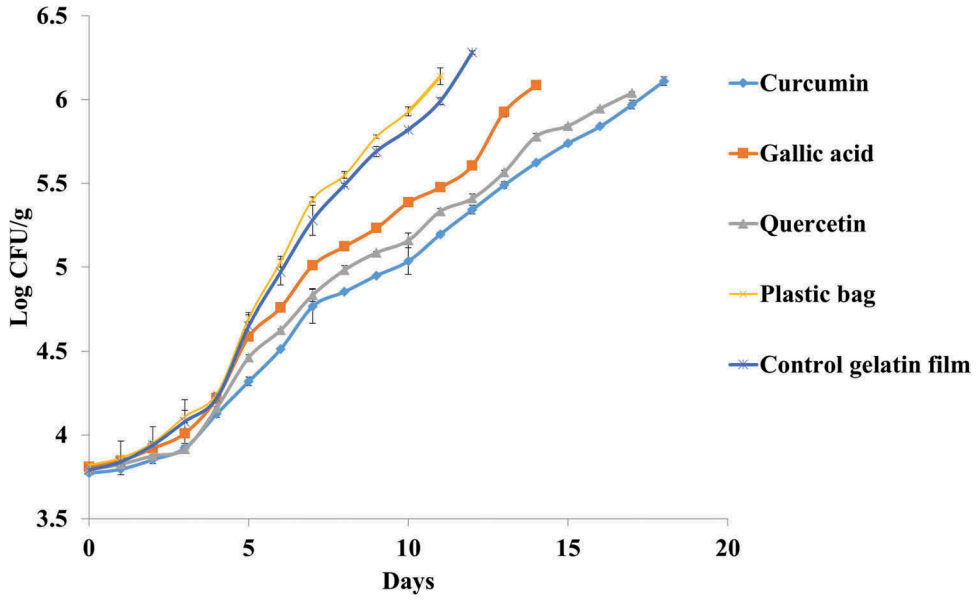

Figure 3. Microbial quality of meat samples packed in 20% NE-loaded edible packaging film.

Figura 3. Calidad microbiana de muestras de carne envasadas en película de embalaje comestible cargada con NE al 20%.

means of cassava starch-based packaging material incorporated with sodium bentonite nanoclay and cinnamon essential oil.

The effect of composite packaging films loaded with NEs on the pH values of broiler meat is shown in Figure S1. The initial pH of fresh broiler meat was 6.01 which was in accordance with the initial pH observed for chicken breast meat (Takma & Korel, 2019). The pH values of the meat samples packaged in both control and active packaging slightly increased during first 7 days of storage and then decreased afterward. A major reason for increase in pH of broiler meat samples might be due to accumulation of metabolites from microbial growth such as ammonia and amines produced by bacteria (Cortez-Vega, Pizato, & Prentice, 2012). The lowest pH of the meat samples was observed in case of plastic (4.48) and control gelatin (4.57) film at the end of storage period (17 days).

4. Conclusion

Raw meat can be easily contaminated due to perishable nature. Due to environmental hazards associated with conventional packaging, there is dire need to replace conventional packaging materials with edible biodegradable active packaging films. Gelatin composite films enriched with polyphenols exhibited antioxidant and antibacterial activity. Therefore, gelatin composite films can be used as active packaging to reduce the microbial load of fresh meat to extend the shelf-life and reduce the risk of food-borne illnesses.

Conflict of interest

The authors declare no conflict of interest.

Funding

This research was supported by Project "Development of packaging materials for nanopreservation of fresh foods" [NRPU, 10413] funded by Higher Education Commission, Pakistan.

References

Ahmed, J., Mulla, M., Arfat, Y. A., Bher, A., Jacob, H., & Auras, R. (2018). Compression molded LLDPE films loaded with bimetallic (Ag-Cu) nanoparticles and cinnamon essential oil for chicken meat packaging applications. *LWT*, *93*, 329–338. doi:10.1016/j.lwt.2018.03.051

Akiyama, H., Fujii, K., Yamasaki, O., Oono, T., & Iwatsuki, K. (2001). Antibacterial action of several tannins against Staphylococcus aureus. *Journal of Antimicrobial Chemotherapy*, *48*(4), 487–491. doi:10.1093/jac/48.4.487

Altiok, D., Altiok, E., & Tihminlioglu, F. (2010). Physical, antibacterial and antioxidant properties of chitosan films incorporated with thyme oil for potential wound healing applications. *Journal of Materials Science: Materials in Medicine*, *21*(7), 2227–2236. doi:10.1007/s10856-010-4065-x

Bhargava, K., Conti, D. S., Da Rocha, S. R., & Zhang, Y. (2015). Application of an oregano oil nanoemulsion to the control of foodborne bacteria on fresh lettuce. *Food Microbiology*, *47*, 69–73. doi:10.1016/j.fm.2014.11.007

Borum, A. E., & Güneş, E. (2018). Antibacterial effect of different concentrations of silver nanoparticles. *Pakistan Veterinary Journal*, *38*, 321–324. doi:10.29261/pakvetj/2018.031.

Cazón, P., Vázquez, M., & Velazquez, G. (2018). Cellulose-glycerol-polyvinyl alcohol composite films for food packaging: Evaluation of water adsorption, mechanical properties, light-barrier properties and transparency. *Carbohydrate Polymers*, *195*, 432–443. doi:10.1016/j.carbpol.2018.04.120

Cazón, P., Vázquez, M., & Velazquez, G. (2019). Composite films with UV-barrier properties based on bacterial cellulose combined with chitosan and poly (vinyl alcohol): study of puncture and water interaction properties. *Biomacromolecules*, *20*(5), 2084–2095. doi:10.1021/acs.biomac.9b00317

Cortez-Vega, W. R., Pizato, S., & Prentice, C. (2012). Quality of raw chicken breast stored at 5C and packaged under different modified atmospheres. *Journal of Food Safety*, *32*(3), 360–368. doi:10.1111/j.1745-4565.2012.00388.x

Cushnie, T. T., & Lamb, A. J. (2005). Antimicrobial activity of flavonoids. *International Journal of Antimicrobial Agents*, *26*(5), 343–356. doi:10.1016/j.ijantimicag.2005.09.002

Dammak, I., De Carvalho, R. A., Trindade, C. S. F., Lourenço, R. V., & Do Amaral Sobral, P. J. (2017). Properties of active gelatin films incorporated with rutin-loaded nanoemulsions. *International Journal of Biological Macromolecules*, *98*, 39–49. doi:10.1016/j.ijbiomac.2017.01.094

Dammak, I., & Sobral, P. J. D. A. (2019). Active gelatin films incorporated with eugenol nanoemulsions: Effect of emulsifier type on films properties. *International Journal of Food Science & Technology*, *54*(9), 2725–2735.

Espitia, P. J. P., Otoni, C. G., & Soares, N. F. F. (2016). Zinc oxide nanoparticles for food packaging applications. In J. Barros-Velázquez, (Ed.), *Antimicrobial food packaging* (pp. 425–431). San Diego, CA: Elsevier. doi:10.1016/B978-0-12-800723-5.00034-6.

Fabra, M. J., Talens, P., & Chiralt, A. (2008). Tensile properties and water vapor permeability of sodium caseinate films containing oleic acid–beeswax mixtures. *Journal of Food Engineering*, *85*(3), 393–400. doi:10.1016/j.jfoodeng.2007.07.022

Gontard, N., & Guilbert, S. T. B. P. H. A. N. E. (1994). Bio-packaging: Technology and properties of edible and/or biodegradable material of agricultural origin. In Mathlouthi, M. (Ed.), *Food packaging and preservation* (pp. 159–181). Boston, MA: Springer.

Hanani, Z. N., Roos, Y. H., & Kerry, J. P. (2014). Use and application of gelatin as potential biodegradable packaging materials for food products. *International Journal of Biological Macromolecules*, *71*, 94–102. doi:10.1016/j.ijbiomac.2014.04.027

Haroun, A. A., & El Toumy, S. A. (2010). Effect of natural polyphenols on physicochemical properties of crosslinked gelatin-based polymeric biocomposite. *Journal of Applied Polymer Science*, *116*(5), 2825–2832.

Hosseini, M. H., Razavi, S. H., & Mousavi, M. A. (2009). Antimicrobial, physical and mechanical properties of chitosan-based films incorporated with thyme, clove and cinnamon essential oils. *Journal of Food Processing and Preservation*, *33*(6), 727–743. doi:10.1111/jfpp.2009.33.issue-6

Iamareerat, B., Singh, M., Sadiq, M. B., & Anal, A. K. (2018). Reinforced cassava starch based edible film incorporated with essential oil and sodium bentonite nanoclay as food packaging material. *Journal of Food Science and Technology*, *55*(5), 1953–1959. doi:10.1007/s13197-018-3100-7

Infante, K., Chowdhury, R., Nimmanapalli, R., & Reddy, G. (2014). Antimicrobial activity of curcumin against food-borne pathogens. *Vedic Research International Biological Medicinal Chemistry*, *2*, 12–19. doi:10.14259/bmc.v2i1

Jafari, S. M., Assadpoor, E., He, Y., & Bhandari, B. (2008). Re-coalescence of emulsion droplets during high-energy emulsification. *Food Hydrocolloids*, *22*(7), 1191–1202. doi:10.1016/j.foodhyd.2007.09.006

Kanmani, P., & Rhim, J. W. (2014). Physicochemical properties of gelatin/silver nanoparticle antimicrobial composite films. *Food Chemistry*, *148*, 162–169. doi:10.1016/j.foodchem.2013.10.047

Karbowiak, T., Debeaufort, F., Champion, D., & Voilley, A. (2006). Wetting properties at the surface of iota-carrageenan-based edible films. *Journal of Colloid and Interface Science*, *294*(2), 400–410. doi:10.1016/j.jcis.2005.07.030

Liang, G., Yang, S., Jiang, L., Zhao, Y., Shao, L., Xiao, J., … Li, X. (2008). Synthesis and anti-bacterial properties of mono-carbonyl analogues of curcumin. *Chemical and Pharmaceutical Bulletin*, *56*(2), 162–167. doi:10.1248/cpb.56.162

Ma, W., Tang, C. H., Yin, S. W., Yang, X. Q., Wang, Q., Liu, F., & Wei, Z. H. (2012). Characterization of gelatin-based edible films incorporated with olive oil. *Food Research International*, *49*(1), 572–579. doi:10.1016/j.foodres.2012.07.037

Mohanty, C., & Sahoo, S. K. (2010). The in vitro stability and in vivo pharmacokinetics of curcumin prepared as an aqueous nanoparticulate formulation. *Biomaterials*, *31*(25), 6597–6611. doi:10.1016/j.biomaterials.2010.04.062

Muyonga, J. H., Cole, C. G. B., & Duodu, K. G. (2004). Fourier transform infrared (FTIR) spectroscopic study of acid soluble collagen and gelatin from skins and bones of young and adult Nile perch (Lates niloticus). *Food Chemistry*, *86*(3), 325–332. doi:10.1016/j.foodchem.2003.09.038

Oussalah, M., Caillet, S., Saucier, L., & Lacroix, M. (2007). Inhibitory effects of selected plant essential oils on the growth of four pathogenic bacteria: E. coli O157: H7, Salmonella typhimurium, Staphylococcus aureus and Listeria monocytogenes. *Food Control*, *18*(5), 414–420. doi:10.1016/j.foodcont.2005.11.009

Pranoto, Y., Rakshit, S. K., & Salokhe, V. M. (2005). Enhancing antimicrobial activity of chitosan films by incorporating garlic oil, potassium sorbate and nisin. *LWT-Food Science and Technology*, *38*(8), 859–865. doi:10.1016/j.lwt.2004.09.014

Rodríguez, M., Oses, J., Ziani, K., & Mate, J. I. (2006). Combined effect of plasticizers and surfactants on the physical properties of starch based edible films. *Food Research International*, *39*(8), 840–846. doi:10.1016/j.foodres.2006.04.002

Sadiq, M. B., Hanpithakpong, W., Tarning, J., & Anal, A. K. (2015). Screening of phytochemicals and in vitro evaluation of antibacterial and antioxidant activities of leaves, pods and bark extracts of Acacia nilotica (L.) Del. *Industrial Crops and Products*, *77*, 873–882. doi:10.1016/j.indcrop.2015.09.067

Sari, T. P., Mann, B., Kumar, R., Singh, R. R. B., Sharma, R., Bhardwaj, M., & Athira, S. (2015). Preparation and characterization of nanoemulsion encapsulating curcumin. *Food Hydrocolloids*, *43*, 540–546. doi:10.1016/j.foodhyd.2014.07.011

Shrestha, S., Sadiq, M. B., & Anal, A. K. (2018). Culled banana resistant starch-soy protein isolate conjugate based emulsion enriched with astaxanthin to enhance its stability. *International Journal of Biological Macromolecules*, *120*, 449–459. doi:10.1016/j.ijbiomac.2018.08.066

Skroza, D., Šimat, V., Smole Možina, S., Katalinić, V., Boban, N., & Generalić Mekinić, I. (2019). Interactions of resveratrol with other phenolics and activity against food-borne pathogens. *Food Science & Nutrition, 7*(7), 2312–2318.

Son, H. Y., Lee, M. S., Chang, E., Kim, S. Y., Kang, B., Ko, H., … Kim, Y. (2019). Formulation and characterization of quercetin-loaded oil in water nanoemulsion and evaluation of hypocholesterolemic activity in rats. *Nutrients*, *11*(2), 244. doi:10.3390/nu11020244

Sood, S., Jain, K., & Gowthamarajan, K. (2014). Optimization of curcumin nanoemulsion for intranasal delivery using design of experiment and its toxicity assessment. Colloids and Surfaces B. *Colloids and Surfaces B: Biointerfaces*, *113*, 330–337. doi:10.1016/j.colsurfb.2013.09.030

Tajbakhsh, S., Mohammadi, K., Deilami, I., Zandi, K., Fouladvand, M., Ramedani, E., & Asayesh, G. (2008). Antibacterial activity of indium curcumin and indium diacetylcurcumin. *African Journal of Biotechnology*, *7*(21), 3832–3835.

Takma, D. K., & Korel, F. (2019). Active packaging films as a carrier of black cumin essential oil: Development and effect on quality and shelf-life of chicken breast meat. *Food Packaging and Shelf Life*, *19*, 210–217. doi:10.1016/j.fpsl.2018.11.002

Trimoulinard, A., Beral, M., Henry, I., Atiana, L., Porphyre, V., Tessier, C., … Cardinale, E. (2017). Contamination by Salmonella spp., Campylobacter spp. and Listeria spp. of most popular chicken- and pork-sausages sold in Reunion Island. *International Journal of Food Microbiology*, *250*, 68–74. doi:10.1016/j.ijfoodmicro.2017.03.017

Wang, L. Z., Liu, L., Holmes, J., Kerry, J. F., & Kerry, J. P. (2007). Assessment of film-forming potential and properties of protein and polysaccharide-based biopolymer films. *International Journal of Food Science & Technology*, *42*(9), 1128–1138. doi:10.1111/ifs.2007.42.issue-9

World Health Organization. (2015). WHO estimates of the global burden of foodborne diseases: Foodborne disease burden epidemiology reference group 2007-2015 (No. 9789241565165). Author.

Zheng, W., & Wang, S. Y. (2001). Antioxidant activity and phenolic compounds in selected herbs. *Journal of Agricultural and Food Chemistry*, *49*(11), 5165–5170. doi:10.1021/jf010697n

Zorofchian Moghadamtousi, S., Abdul Kadir, H., Hassandarvish, P., Tajik, H., Abubakar, S., & Zandi, K. (2014). A review on antibacterial, antiviral, and antifungal activity of curcumin. *BioMed Research International*, *2014*. doi:10.1155/2014/186864.